# Unsteady Heat Transfer on Turbine Blades

Tuncer Cebeci*
*California State University, Long Beach, California*
Robert J. Simoneau†
*NASA Lewis Research Center, Cleveland, Ohio*
and
Max F. Platzer‡
*Naval Postgraduate School, Monterey, California*

**This paper describes a method for calculating heat transfer on turbine blades subjected to passing wakes. It is based on the numerical solution of the boundary-layer equations for laminar, transitional, and turbulent flows with a novel procedure to account for the movement of the stagnation point. Results are presented for a model flow and show that the procedure is numerically sound and produces results that can give good agreement with measurements provided that the turbulence model is adequate.**

## Nomenclature

$C_D$ = drag coefficient of the rotating pin
$d$ = diameter of rotating pin
$D$ = diameter of heated stator
$F$ = blade-passing frequency, Hz
$n$ = number of rotating pins
$Pr$ = Prandtl number
$Pr_t$ = turbulent Prandtl number
$r$ = radial distance from rotation axis
$S$ = separation distance between pins
$St$ = Strouhal number, $DF/u_\infty$
$t$ = time
$T$ = temperature
$u,v$ = velocity components in $x$ and $y$ directions, respectively
$u_\infty$ = freestream velocity
$V_m$ = wake centerline velocity
$x$ = coordinate, measured along the surface
$y$ = coordinate, normal to the surface
$\bar{y}$ = normal-to-rotating pin wake axis
$\delta$ = half-wake width behind rotating pins
$\epsilon_m$ = eddy viscosity
$\eta$ = normalized $y$ coordinate, $\sqrt{u_\infty/\nu D}\, y$
$\nu$ = kinematic viscosity
$\xi$ = normalized $x$ coordinate, $x/D$
$\tau$ = dimensionless time, $tu_\infty/D$
$\psi$ = stream function
$\omega$ = angular velocity of rotating pins

*Subscripts*

$e$ = boundary-layer edge
$\ell$ = laminar
$s$ = stagnation point
$w$ = wall

## I. Introduction

THE influence of the blades of a stator on those of a downstream rotor have been shown, for example, by Dring et al.,[1] Dunn et al.,[2] and Ashworth et al.,[3] to be important, and Hodson[4] and Binder et al.[5] have mapped the convection of wakes through the rotor. The nature of the blade-passing problem can be explained in relation to Fig. 1a which shows that the rotor blade passes through the wake of the upstream stator blade and generates a wake which affects the onset flow to the second stator. In effect, the blades of the rotor and second stator are subjected to a freestream velocity which varies periodically with time and with a random turbulence fluctuation superimposed. These effects may be simulated by the arrangement of Fig. 1b which shows one cylinder of a number arranged on a wheel which rotates upstream of a turbine blade.

A number of approaches to the calculation of these effects have been examined including that of Rai,[6] who solved the time-averaged Navier-Stokes equations with a complex arrangement of patched and overlaid grids and attempted to reproduce the measurements of Dring et al.[1] with some success. An alternative approach is to use boundary-layer theory, which makes use of the solutions of viscous and inviscid equations appropriate to the flows described above, and their coupling by special techniques. The inviscid method must be able to cope with the periodic onset velocities of Fig. 1b and their effects on the blade flow from the stagnation region to the wake and the boundary-layer method with flow reversals associated with the movement of the stagnation point with time and space as well as flow reversal and separation that may occur in the downstream region.

The work described in this paper is directed toward the development of a general method for calculating unsteady heat transfer on turbine blades. As an essential preliminary, we describe a boundary-layer method for calculating heat transfer for prescribed freestream conditions and test it for a model problem which corresponds to the wake-rotor interaction experiment of Refs. 7 and 8 emphasizing the stagnation region. It can readily be combined with an inviscid-flow solution to permit calculations along the full chord of the blade. We assume that the external velocity distribution on the circular cylinder near the stagnation point is represented by the function

$$\frac{u_e}{u_\infty}(x,t) = 2A(t)\left[\frac{2x}{D} + B(t)\right] \tag{1}$$

where $A(t)$ is the variable onset flow and $B(t)$ is the change in flow incidence.

The basic equations and the initial and boundary conditions are considered in the following section, which is followed by a description of the numerical method used to solve the

Received Sept. 14, 1988; revision received March 20, 1989. 

*Professor and Chairman, Aerospace Engineering Department. Fellow AIAA.
†Chief, Heat Transfer Branch.
‡Professor, Department of Aeronautics. Associate Fellow AIAA.

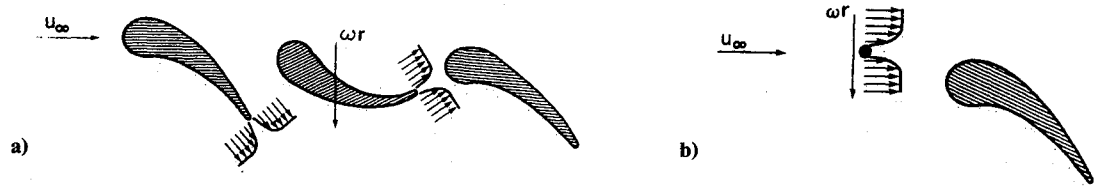


**Fig. 1 Flow configuration: a) turbine stage; and b) simulation.**

boundary-layer equations. Section IV presents the results and discussion, and the paper ends with a summary of the more important conclusions.

## II. Basic Equations

For a specified wall temperature, no mass transfer, and with eddy viscosity $\epsilon_m$ and turbulent Prandtl number $Pr_t$ concepts, the two-dimensional incompressible boundary-layer equations can be written as in Ref. 9:

$$\frac{\partial u}{\partial x}+\frac{\partial v}{\partial y}=0 \tag{2}$$

$$\frac{\partial u}{\partial t}+u\frac{\partial u}{\partial x}+v\frac{\partial u}{\partial y}=\frac{\partial u_e}{\partial t}+u_e\frac{\partial u_e}{\partial x}+\nu\frac{\partial}{\partial y}\left(b_1\frac{\partial u}{\partial y}\right) \tag{3}$$

$$\frac{\partial T}{\partial t}+u\frac{\partial T}{\partial x}+v\frac{\partial T}{\partial y}=\frac{\nu}{Pr}\frac{\partial}{\partial y}\left(b_2\frac{\partial T}{\partial y}\right) \tag{4}$$

$$y=0, \qquad u=v=0, \qquad T=T_w(x) \tag{5a}$$

$$y=\infty, \qquad u=u_e(x,t), \qquad T=T_e \tag{5b}$$

$$b_1=1+\epsilon_m^+, \qquad b_2=1+\frac{Pr}{Pr_t}\epsilon_m^+, \qquad \epsilon_m^+=\epsilon_m/\nu \tag{6}$$

With dimensionless variables $\tau$, $\xi$, $\eta$, $w$, $m$, $G$, together with a dimensionless stream function $f$,

$$\tau=\frac{tu_\infty}{D}, \qquad \xi=\frac{x}{D}, \qquad \eta=\left(\frac{u_\infty}{\nu D}\right)^{1/2}y, \qquad w=\frac{u_e}{u_\infty},$$

$$m=\frac{1}{(T_w-T_e)}\frac{\mathrm{d}\,(T_w-T_e)}{\mathrm{d}\xi}, \qquad G=\frac{T_w-T}{T_w-T_e},$$

$$\psi=(u_\infty\nu D)^{1/2}f(\xi,\eta,\tau) \tag{7}$$

Eqs. (2–5) become

$$(b_1f'')'+f''\theta+\frac{\partial w}{\partial\tau}+w\frac{\partial w}{\partial\xi}=\frac{\partial f'}{\partial\tau}+f'\frac{\partial f^1}{\partial\xi} \tag{8}$$

$$(b_2G')'+G'\theta+m(1-G)f'=\frac{\partial G}{\partial\tau}+f'\frac{\partial G}{\partial\xi} \tag{9}$$

$$\eta=0, \qquad f=f'=0, \qquad G=0 \tag{10a}$$

$$\eta=\eta_e, \qquad f'=w, \qquad G=1 \tag{10b}$$

where

$$\theta=\frac{\partial f}{\partial\xi} \tag{11}$$

Since the representation of transition is essential to the present problem, we have preferred to use the algebraic eddy-viscosity approach of Cebeci and Smith,[10] which is known to represent transition adequately. A constant value of unity has been assumed for $Pr_t$.

The initial conditions required for the above system can be arbitrary or can be obtained by solving the steady-state form of the equations. Here we use the latter approach and write

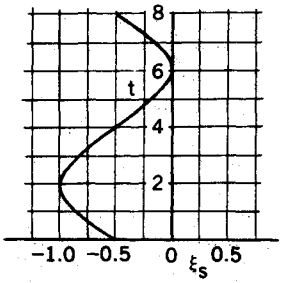


**Fig. 2 Variation of the stagnation point with time according to Eq. (1).**

Eqs. (8) and (9) in the form:

$$(b_1f'')'+f''\theta+w\frac{\partial w}{\partial\xi}=f'\frac{\partial f'}{\partial\xi} \tag{12}$$

$$(b_2G')'+G'\theta+m\,(1-G)f'=f'\frac{\partial G}{\partial\xi} \tag{13}$$

Initial conditions for these equations correspond to laminar flow, which admits a similarity solution at the stagnation point. The transitional and turbulent flow calculations can be started at any location away from the stagnation point by specifying the location of the onset of transition.

The calculation of upstream boundary conditions in the $(t,y)$ plane at some $x=x_o$, when the conditions at a previous time line are known, can introduce problems. To illustrate this for the case of a moving stagnation point, consider Eq. (1). Since $u_e=0$ at the stagnation point by definition, its location $\xi_s$ based on the external streamlines is given by

$$2\xi_s=-B(t) \tag{14}$$

Figure 2 shows the variation of the stagnation point with time according to Eq. (1) with $B(t)=1+c\sin\omega t$, where $c=1$ and $\omega=\pi/4$. We see that the stagnation point $\xi_s$ is at $-1$ when $t=2$, and at 0 when $t=6$, etc. If $\xi_s$ were fixed, we could assume that $u=0$, at $\xi=\xi_s$ for all time and for all $\eta$, but this is not the case. It is also possible to assume that the stagnation point is coincident with zero $u$ velocity for a prescribed time but we should note that the stagnation point given by Eq. (14) is based on vanishing external velocity. For a time-dependent flow, this does not necessarily imply that the $u$ velocity is zero across the the layer for a given $\xi$ location and specified time; flow reversals do occur due to the movement of the stagnation point and cause the locus of zero $u$ velocity to vary with $x$ requiring the use of the characteristic box method, as discussed in Ref. 11 and in the following section.

## III. Numerical Method

The equations of the previous section are solved with the box scheme of Keller,[12] which is used in two forms depending on the presence or otherwise of reverse flow. The regular box scheme is used where the flow is always in the streamwise direction, and the characteristic box scheme is used where there are negative streamwise velocities and also to generate the upstream boundary conditions.

To solve the momentum equation for steady-state conditions subject to its boundary conditions, we let $f' = e$ and introduce a new function $g$ defined by

$$e' = g \tag{15a}$$

and, with $b_1 = b_1$, write Eqs. (11–12) and their boundary conditions as

$$\theta' = \frac{\partial e}{\partial \xi} \tag{15b}$$

$$(b_1 g)' + g\theta + w\frac{\partial w}{\partial \xi} = e\frac{\partial e}{\partial \xi} \tag{15c}$$

$$\eta = 0, \quad e = \theta = 0, \quad \eta = \eta_e, \quad e = w \tag{16}$$

To write the difference equations, we consider a net rectangle in which the net points are denoted by

$$\xi_o = 0, \quad \xi_i = \xi_{i-1} + r_i, \quad i = 1,2,\ldots,I$$

$$\eta_o = 0, \quad \eta_j = \eta_{j-1} + h_j, \quad j = 1,2,\ldots,J \tag{17}$$

The finite-difference approximations to Eqs. (15a) are obtained by averaging about the midpoint $(\xi_i, \eta_{j-1/2})$

$$h_j^{-1}(e_j^i - e_{j-1}^i) = g_{j-1/2}^i \equiv \tfrac{1}{2}(g_j^i + g_{j-1}^i) \tag{18}$$

and those to Eqs. (15b,15c) by centering all quantities except $\theta$ at the center of the rectangle $(\xi_{i-1/2}, \eta_{j-1/2})$ and taking the values of each, say, $e$, at the corners of the box, that is,

$$e_{j-1/2}^{i-1/2} = \frac{1}{2}(e_{j-1/2}^i + e_{j-1/2}^{i-1}) = \frac{1}{4}(e_j^i + e_{j-1}^i + e_j^{i-1} + e_{j-1}^{i-1}) \tag{19a}$$

The centering of $\theta$ is achieved as

$$\theta_{j-1/2}^{i-1/2} = \frac{1}{2}(\theta_j^{i-1/2} + \theta_{j-1}^{i-1/2}) \equiv \frac{1}{2}(\theta_j + \theta_{j-1}) \tag{19b}$$

In this notation, the difference approximations to Eqs. (15b,15c) can be written in the form:

$$h_j^{-1}(\theta_j - \theta_{j-1}) = r_i^{-1}(e_{j-1/2}^i - e_{j-1/2}^{i-1}) \tag{20a}$$

$$h_j^{-1}(b_j^i g_j^i - b_{j-1}^i g_{j-1}^i) + g_{j-1/2}^i \theta_{j-1/2} + g_{j-1/2}^{i-1}\theta_{j-1/2} - r_i^{-1}(e^2)_{j-1/2}^i = R_{j-1/2}^{i-1} \tag{20b}$$

where

$$R_{j-1/2}^{i-1} = -\Big\{h_j^{i-1}(b_j^{i-1}g_j^{i-1} - b_{j-1}^{i-1}g_{j-1}^{i-1}) + r_i^{-1}\Big[(w^2)_{j-1/2}^i - (w^2)_{j-1/2}^{i-1} + (e^2)_{j-1/2}^{i-1}\Big]\Big\} \tag{21}$$

The boundary conditions of Eq. (16) become

$$e_o = \theta_o = 0, \quad e_j = w_j \tag{22}$$

The regular box scheme is well known and the reader is referred to Ref. 11 for details. The characteristic box scheme makes use of the definition

$$d\tau = \frac{d\xi}{e} \tag{23}$$

If we denote the distance along a streamline by $s$ and the angle that the streamline makes with the $\tau$ axis by $\beta$ (see Fig. 3), then Eq. (8) in terms of variables $e$ and $g$ becomes

$$(bg)' + g\theta + \frac{\partial w}{\partial \tau} + w\frac{\partial w}{\partial \xi} = \lambda\frac{\partial e}{\partial s} \tag{24}$$

where

$$\lambda = \sqrt{(1+e^2)} \tag{25a}$$

$$\beta = \tan^{-1} e \tag{25b}$$

The solution procedure for Eqs. (15a,15b) and (24) and their boundary conditions with the characteristic box scheme is similar to that of the regular box scheme, and since we consider a three-dimensional form of the equation, we also consider the net points

$$\tau_o = 0, \quad \tau_n = \tau_{n-1} + k_n, \quad n = 1,2,\ldots,N \tag{26}$$

To obtain the solutions on the first time line $\tau_1$, we assume that the stagnation line based on the external streamline is given, the solution of point 1 is known, and direct our attention to point 2. The finite-difference approximations to Eq. (24) are written along the streamline direction (see Fig. 3) at point $p$:

$$\frac{h_j^{-1}}{2}(b_j^{i,n}g_j^{i,n} - b_{j-1}^{i,n}g_{j-1}^{i,n}) + \frac{h_j^{-1}}{2}(b_j^{m,n-1}g_j^{m,n-1} - b_{j-1}^{m,n-1}g_{j-1}^{m,n-1}) + \frac{1}{2}(g_{j-1/2}^{i,n} + g_{j-1/2}^{m,n-1})\theta_{j-1/2}^P + \frac{\partial w}{\partial \tau}(P) + w\frac{\partial w}{\partial \xi}(P) = \frac{1}{2}(\lambda_{j-1/2}^{i,n} + \lambda_{j-1/2}^{m,n-1} + \lambda_{j-1/2}^{m,n-1})\frac{e_{j-1/2}^{i,n} - e_{j-1/2}^{m,n-1}}{\Delta s_{j-1/2}} \tag{27}$$

where

$$\Delta s_{j-1/2} = \frac{k_n}{\cos\beta_{j-1/2}} \tag{28}$$

The relationship between $\theta_{j-1/2}^P$ and the values of $\theta$ centered at $(i-1/2, n-1/2)$ and $(i-3/2, n-1/2)$ is

$$\theta_{j-1/2}^P = \frac{\theta_{j-1/2}^i - \theta_{j-1/2}^{i-1/2}}{\xi_{i-3/2} - \xi_{i-1/2}}(\xi^P - \xi_{i-3/2}) + \theta_{j-1/2}^{i-3/2} \tag{29}$$

As discussed in Ref. 11, Eqs. (18), (20a), and (27) and their boundary conditions are linearized by Newton's method and solved with the block-elimination method.

To generate the upstream boundary conditions, we assume that the first profile on either side of the "edge" stagnation point is known. In the presence of flow reversal at, say, point 2 of Fig. 3, an extension of the characteristic scheme is used on an iterative basis. When there is no flow reversal, then the regular box scheme is used. Further details of the method and its application are provided in Ref. 11.

## IV. Results and Discussion

The numerical method of the previous section is used to obtain the solutions of the continuity, momentum, and energy equations for the experimental rotor-wake model of Refs. 7 and 8 in order to compare the calculations for turbulent flows with measurements. Figure 4 shows the flow configuration and the notation. For a time period $t_g$, the cylinder is subjected to a freestream velocity $u_\infty$, and for $t_w$ it is immersed in a superimposed rotating wake that has a rotational component $\omega r$. The cycle repeats itself with a blade-passing frequency $F[\equiv 1/(t_g + t_w)]$ and is related to the Strouhal number $St$ by $FD/u_\infty$. Dimensionless expressions for the parameters $A(\tau)$ and $B(\tau)$ needed in Eq. (1) to define the external velocity distribution near the stagnation region are obtained by using the procedure described in Ref. 13. With $n$ denoting the number of rotating pins, $St = 2n/\pi\ (D/r)(\omega r/u_\infty)$, $A$ and $B$ are written as

$$A(\tau) = [f^2 + E_2^2\,(St)^2(1-f)^2]^{1/2} \tag{30}$$

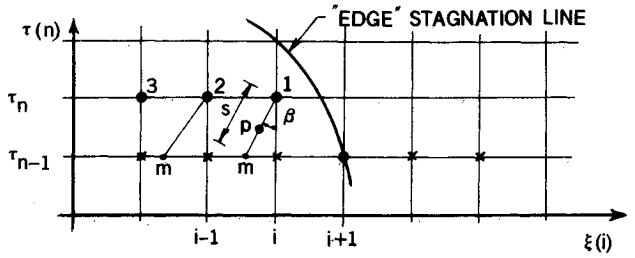


**Fig. 3 Notation and grid for the characteristic box scheme (for details see Ref. 11).**

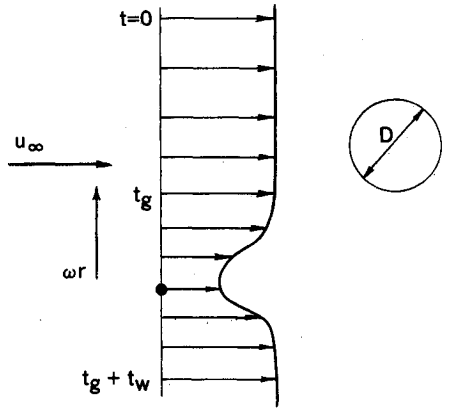


**Fig. 4 Notation and flow configuration.**

$$B(\tau) = \tan^{-1}\left[E_2 St\left(\frac{1-f}{f}\right)\right] \tag{31}$$

with $f$ and $E_2$ given by

$$f(\tau) = \frac{1+V_m}{2} - \frac{1-V_m}{2}\cos[\pi(\bar{y}/\delta)], \qquad E_2 = \frac{2\pi r}{nD} \tag{32}$$

$$\frac{\bar{y}}{\delta} = 1 - E_1\frac{\tau St}{[1+E_2^2 St^2]^{1/2}}, \qquad E_1 = \frac{2E_2}{1.132(C_D\, d/D\, S/D)^{1/2}} \tag{33}$$

The calculations were first performed for a laminar flow to test the numerical procedure. With the choice of $E_2 = \sqrt{10}$, $E_1 = 10$, and $V_m = 1/3$, the parameters $A$, $B$, and $f$ in Eqs. (30-32) become

$$A(\tau) = [f^2 + 10(St)^2(1-f)^2]^{1/2} \tag{34}$$

$$B(\tau) = \tan^{-1}\left[\sqrt{10}\, St\left(\frac{1-f}{f}\right)\right] \tag{35}$$

$$f = \frac{2}{3} - \frac{1}{3}\cos[\pi(1 - 10\, St\tau)] \tag{36}$$

The computed values of wall heat flux $G'(0)$ for two values of Strouhal number show that they are not influenced by the changes in the freestream velocity and are virtually constant for the range of $\xi$ and $\tau$ values considered, with $G'(0) \sim 0.50$ for $St = 0.1$ and $G'(0) \sim 0.51$ for $St = 0.2$. On the other hand, as shown in Fig. 5, the computed values of wall shear $f''(0)$ for $St = 0.1$ are influenced by the changes in the freestream velocity that cause flow reversals in the velocity profiles around the stagnation point based on the vanishing of the external velocity. The movement of the stagnation point and the resulting flow reversals increase with time and with space so that, for example, the calculations for steady state

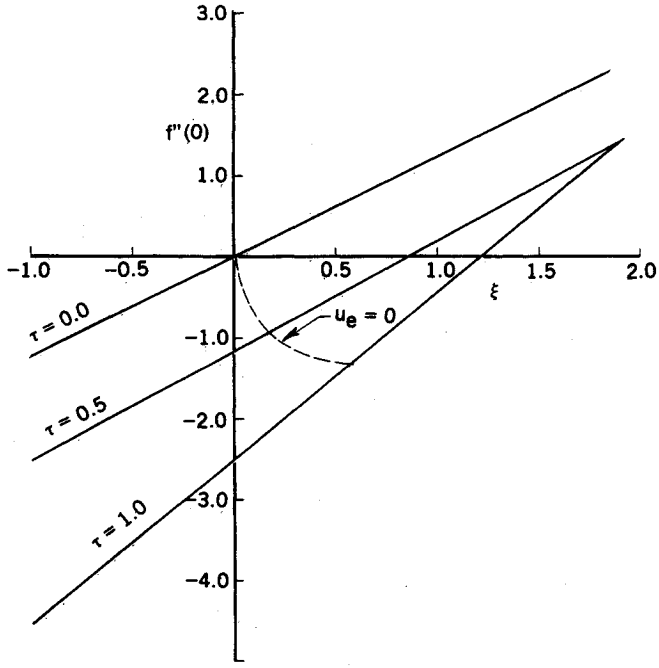


**Fig. 5 Variation of the wall shear parameter $f''(0)$ with $\xi$ ($St = 0.10$).**

have the stagnation point at $\xi = 0$, and, as expected, there is no flow reversal on either side of the stagnation point. At $\tau = 0.5$, the stagnation point moves to $\xi = 0.15$, but the flow reversals in the velocity profiles continue up to and including $\xi = 0.85$ as can be seen from the results shown in Fig. 5. At $\tau = 1.0$, the stagnation point has moved to $\xi = 0.55$ but the flow reversals persist for a longer distance and continue until $\xi = 1.20$. As can be seen from the velocity profiles in Fig. 6, the region of flow reversal across the layer has now increased and is substantially more pronounced than at $\tau = 0.5$. The wall shear and displacement thickness results for $St > 0.2$ show similar trends and, as expected, the flow reversals in the velocity profiles, for example at $\tau = 1.0$, are bigger than those at $St = 0.1$ but cover the same range in $\xi$.

These laminar-flow results confirm that the numerical procedure is able to obtain solutions for a range of blade-passing frequencies of practical relevance. The movements of the stagnation point cause no computational difficulties, and the numerical tests show that the accuracy is better than required for practical problems.

The present method is applicable to laminar, transitional, and turbulent flows. It requires that the calculations start as laminar from the stagnation point. The onset of transition can be assigned to occur in accordance with experiments and the subsequent transitional and turbulent flows represented by the algebraic eddy-viscosity model of Cebeci and Smith[10] in which the length of the transitional region depends upon the freestream conditions.

In the case of turbulent flow, estimates of $E_1$, $E_2$, and $V_m$ can be obtained from the experiments of Ref. 7 with $D = 12.7$ mm, $d = 3.18$ mm, $S = 25.4$ mm, $r = 16.925$ cm, $C_D = 1.2$, $n = 24$, and $V_m = 0.62$, so that $E_1 = 7.9$, $E_2 = 3.49$, and

$$A(\tau) = [f^2 + (3.49)^2(St)^2(1-f^2)]^{1/2} \tag{37}$$

$$B(\tau) = \tan^{-1}\left[3.49\left(\frac{1-f}{f}\right)\right] \tag{38}$$

$$f = 0.81 - 0.19\cos[\pi(1 - 7.9\, St\tau)] \tag{39}$$

The turbulent-flow calculations were performed in the above manner to simulate the near stagnation region of the flow of Refs. 7 and 8. The onset of transition was set very

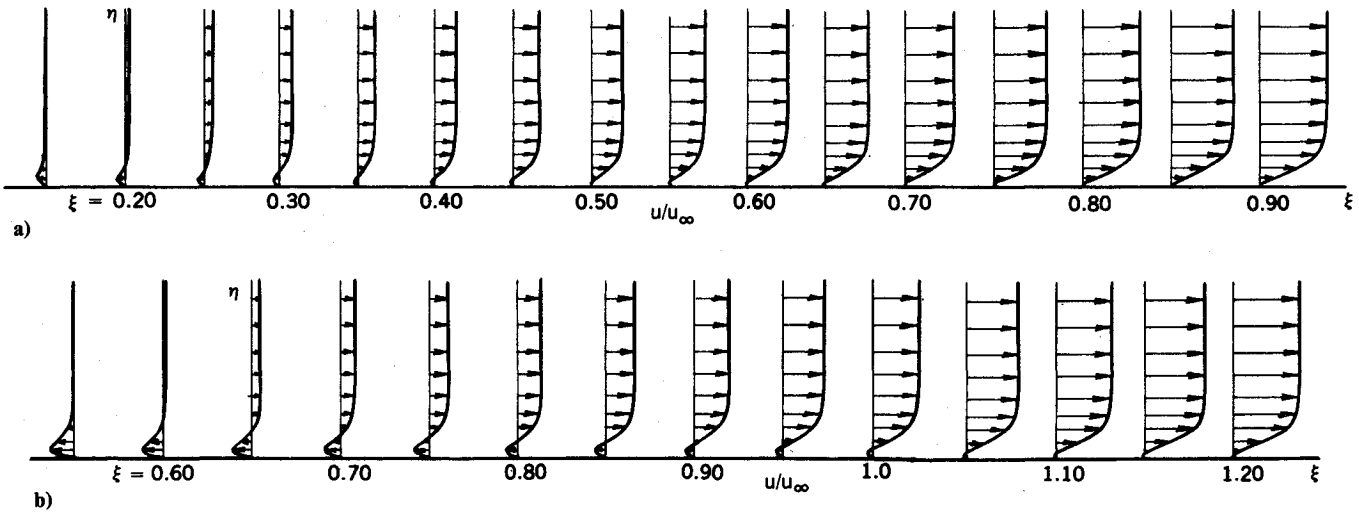


**Fig. 6 Variation of the velocity profiles near the stagnation region for two values of time: a) $\tau = 0.5$; and b) $\tau = 1.0$.**

close to the stagnation point and transitional- and turbulent-flow calculations were performed for $0 \le t \le (t_w + t_g)$, for one cycle for the experimental Reynolds number of $R_d = 76{,}000$. Since the experimental data suggests that the average Nusselt number is relatively constant and is 10% higher than that of laminar flow, it was assumed that the transitional region was negligibly short. Futhermore, the present eddy-viscosity model is a function of the velocity field and the heat-transfer parameter is relatively constant in the stagnation region $0 \le \theta \le 40$ deg, so that it was further assumed that the eddy viscosity in this region be constant. This implies that the distribution of eddy viscosity determined at the end of the transitional region ($\gamma_{tr} = 1$) retains the same numerical value throughout the turbulent-flow calculations. As a consequence of the above, the ratios of the average Nusselt number $Nu$ on the blade passing a wake to that of a blade in a freestream during one cycle, $Nu_s$, used in the presentation of the experimental results were calculated from

$$\frac{Nu}{Nu_s} = \frac{Nu_b + Nu_g}{Nu_s} = \frac{\int_o^{t_w} Nu\,dt + \int_{t_w}^{t_g + t_w} Nu_t dt}{\int_0^{t_g + t_w} Nu_t dt} \tag{40}$$

Since the cycle time is $(t_w + t_g)$, the numerator of Eq. (40) contains two parts: one for the blade submerged in the wake, $Nu_b$, and the other for the base in a freestream, $Nu_g$, during time $t_g$ where the flow is laminar and admits similarity. In the transformed coordinates of the calculations, the ratio of the averaged Nusselt number may be written as

$$\frac{Nu}{Nu_s} = \frac{\int_0^{2\pi} G'_w\,d\tau + (G'_w)_\ell t_g}{(G'_w)_\ell (t_g + t_w)} \tag{41}$$

where $(G'_w)_\ell = 1.0034$ for laminar flows. The measured and calculated values of average Nusselt-number ratios were found to be 1.1 and 1.09, respectively, and constant throughout the turbulent-flow region. The closeness of the two results is gratifying but should be viewed with caution, bearing in mind the assumptions that have been made in relation to the eddy-viscosity model and the assumed freestream velocity distribution. Alternative approaches to the representation of the turbulence characteristics of the stagnation region have been examined, for example by Taulbee and Tran,[13] and deserve future consideration. In addition, the integration of the heat-transfer parameter $G'_w$ is subject to some uncertainty in the blending region between laminar and turbulent flows.

## V. Concluding Remarks

The preceding sections describe essential steps in the development of a general method for the calculation of unsteady heat transfer on turbine blades. It has emphasized the stagnation region since this must be correctly represented in order for the method to calculate the flow and heat-transfer characteristics of a blade passage. This region involves a moving stagnation point with consequent reverse flows and has required the development and use of a novel numerical procedure to solve the equations for conservation of mass, momentum, and energy. The characteristic box scheme, with its stability requirements, has been used in regions of reverse flow, and the regular box scheme elsewhere. Transitional and turbulent flow have been represented by an eddy-viscosity formula.

The method has been applied to a model problem for which heat-transfer measurements have been reported and calculations are performed to include the transitional- and turbulent-flow regions. The results confirm that the method represents the essential features of the flow, including the averaged Nusselt number in close agreement with the measured value. The method can now be extended to include procedures for the solution of the unsteady, inviscid-flow equations and to ensure interaction between the inviscid and boundary-layer flows. Both procedures are available so that the general method can be assumed and applied to blade-passage flows.

## References

[1]Dring, R. P., Joslyn, H. D., Hardin, L. W., and Wagner, J. H., "Turbine Rotor-Stator Interaction," *Journal of Engineering for Power*, Vol. 104, No. 4, 1982, pp. 729–742.

[2]Dunn, M. G., George, W. K., Rae, W. J., Moller, J. C., Woodward, S. H., and Seymour, P. J., "Heat-Flux Measurements for the Rotor of a Full-Stage Turbine, Pt. II: Description of Analysis Technique and Typical Time Resolved Measurements," American Society of Mechanical Engineers Paper 86-GT-78, June 1986.

[3]Ashworth, D. A., LaGraff, J. E., Schultz, D. L., and Grinrod, K. J., "Unsteady Aerodynamic and Heat-Transfer Processes in a Transonic Turbine Stage," *Journal of Engineering for Power*, Vol. 107, No. 4, Oct. 1985, pp. 1022–1030.

[4]Hodson, H. P., "Measurements of Wake-Generated Unsteadiness in the Rotor Passages of Axial Flow Turbines," *Journal of Engineering for Power*, Vol. 7, No. 2, 1985, pp. 467–476.

[5]Binder, A., Forster, W., Kruse, H., and Rogge, H., "An Experimental Investigation into the Effect of Wakes on the Unsteady Turbine Rotor Flow," *Journal of Engineering for Power*, Vol. 7, No. 2, 1985, pp. 458–466.

[6]Rai, M. M., "Navier-Stokes Simulations of Rotor-Stator Interaction Using Patched and Overlaid Grids," AIAA Paper 85-1519, July 1985.

[7]O'Brien, J. E., Simoneau, R. J., LaGraff, J. E., and Morehouse, K. A., "Unsteady Heat Transfer and Direct Comparison to Steady-State Measurements in a Rotor-Wake Experiment," *Proceedings of the 8th International Heat-Transfer Conference*, Aug. 1986; also NASA TM-87220.

[8]Morehouse, K. A. and Simoneau, R. J., "Effect of a Rotor Wake on the Local Heat Transfer on the Forward Half of a Circular Cylinder," *Proceedings of the 8th International Heat-Transfer Conference*, Aug. 1986; also NASA TM-87234.

[9]Cebeci, T. and Bradshaw, P., *Physical and Computational Aspects of Convective Heat Transfer*, Springer-Verlag, New York, 1984.

[10]Cebeci, T. and Smith, A. M. O., *Analysis of Turbulent Boundary Layers*, Academic, New York, 1974.

[11]Cebeci, T. and Platzer, M. F., "A General Method for Unsteady Heat Transfer in Turbine Blades," NASA CR 4206, 1989.

[12]Keller, H. B., "Numerical Methods in Boundary-Layer Theory," *Annual Review of Fluid Mechanics*, Vol.10, 1978, pp. 417-433.

[13]Taulbee, D. B. and Tran, L., "Stagnation Streamline Turbulence," *AIAA Journal*, Vol. 26, No. 8, 1988, pp. 1011-1013.